# Electronic Supporting Information for

**Few-layered $V_2C$ MXene derived 3D $V_3S_4$ nanocrystals functionalized carbon flakes boosting polysulfide adsorption and catalytic conversion towards Li-S batteries**

*Zhaolin Tan, Sen Liu, Xu Zhang, Jingxuan Wei, Yang Liu,* Linrui Hou* and Changzhou Yuan**

School of Materials Science & Engineering, University of Jinan, Jinan, 250022, P. R. China

E-mail: ayuancz@163.com; mse_yuancz@ujn.edu.cn

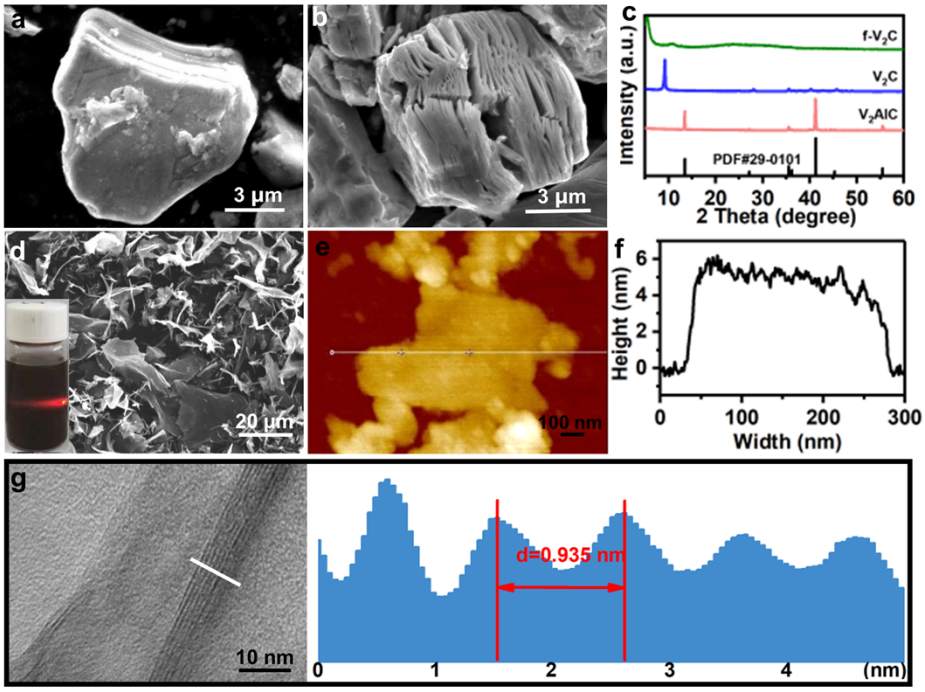


**Fig. S1** SEM image of (a) $V_2AlC$ and (b) multi-layered $V_2C$ MXene; (c) XRD patterns of $V_2AlC$, $V_2C$ and f-$V_2C$. (d) FESEM image, (e) AFM images and (f) corresponding height profile, and HRTEM image of f-$V_2C$. The inset in panel (d) is the digital photograph for the Tyndall effect of the f-$V_2C$ colloidal solution.

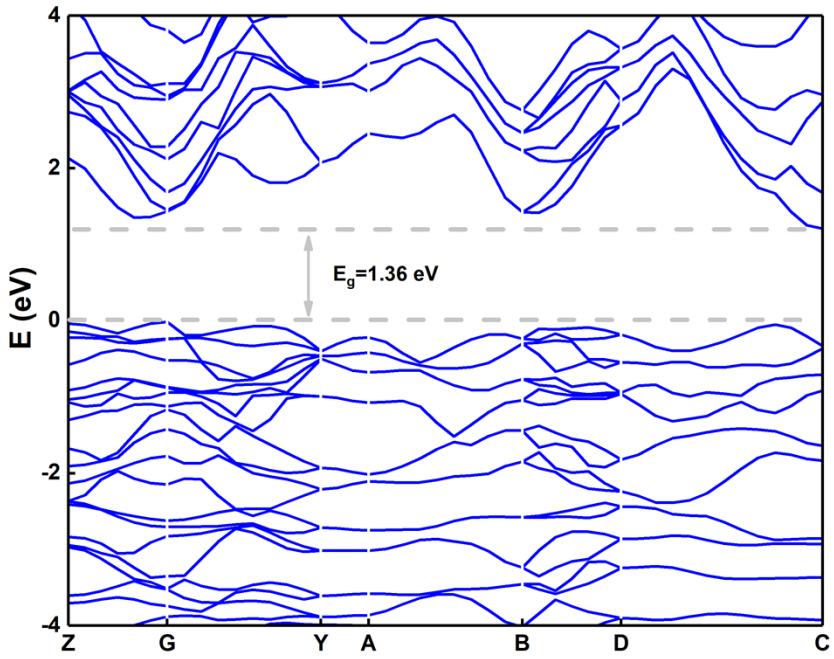


**Fig. S2** Band structure of $V_3S_4$.

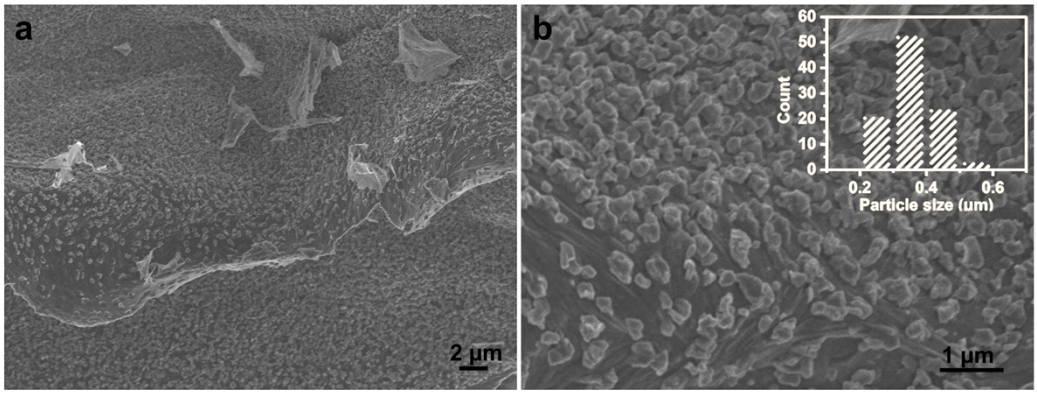


**Fig. S3** (a, b) FESEM images with different magnifications of the $V_3S_4$@C-8 and particle size distribution diagram (the inset in panel b) diagram derived from the panel (b).

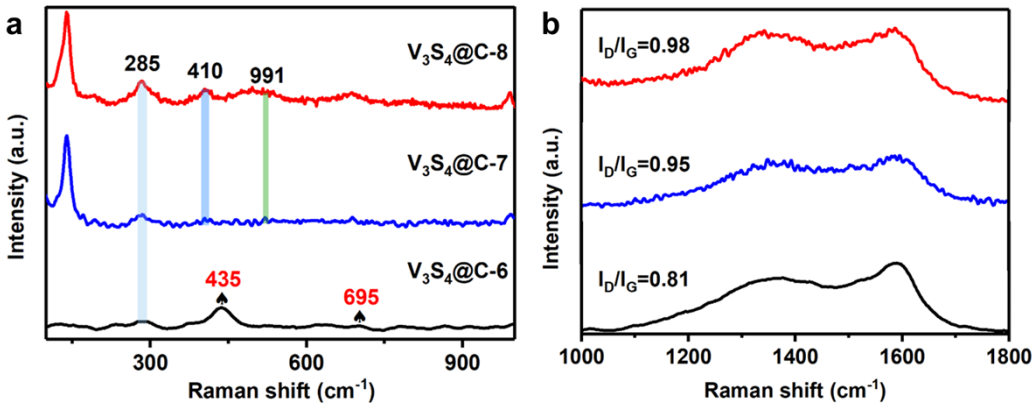


**Fig. S4** (a, b) Raman spectra of $V_3S_4$@C-6, $V_3S_4$@C-7, and $V_3S_4$@C-8.

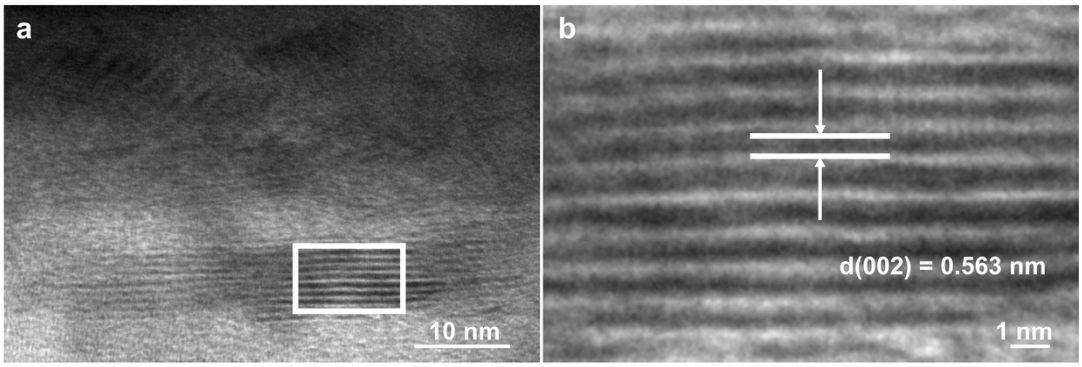


**Fig. S5** (a) TEM and (b) HRTEM images of the (002) lattice of $V_3S_4$.

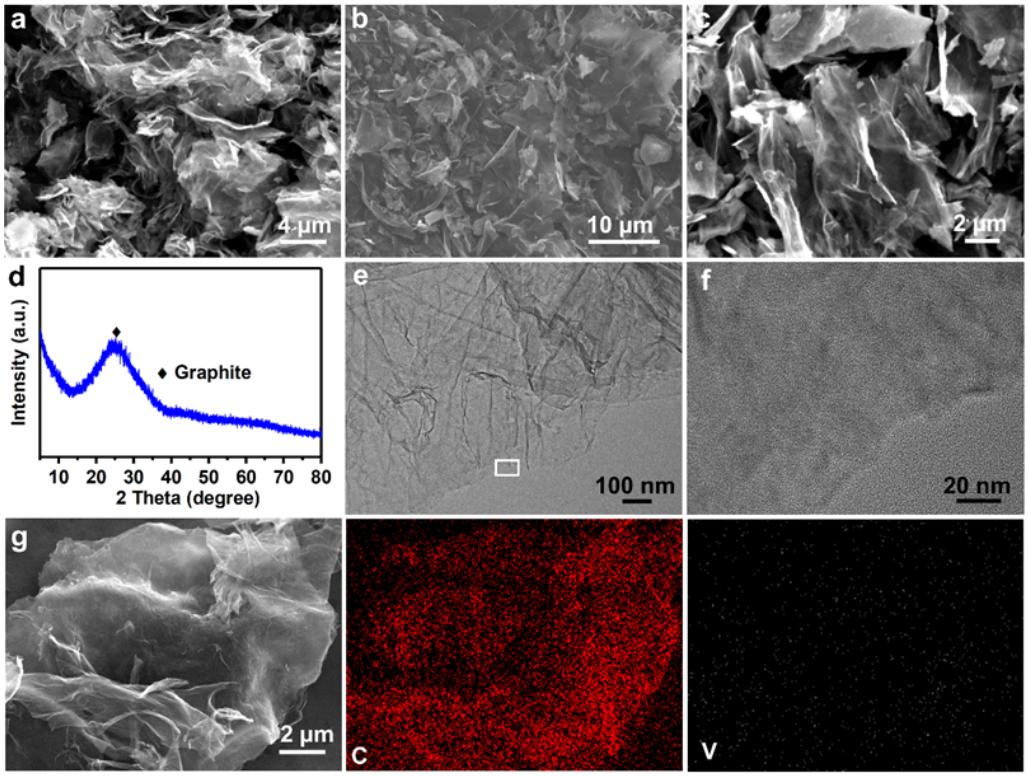


**Fig. S6** FESEM images of (a) $V_3S_4$@C-6, (b) $V_3S_4$@C-7 and (c) $V_3S_4$@C-8 after treated by HCl; (d) XRD pattern, (e, f) TEM images, (g) SEM image and corresponding EDS elemental mapping images of $V_3S_4$@C-7 after treated by HCl.

**Table S1** Mass of Samples before and after HCl treatment

| Sample | Before HCl treatment | After HCl treatment |
|---|---|---|
| $V_3S_4$@C-6 | 30 mg | 5.3 mg |
| $V_3S_4$@C-7 | 30 mg | 2.3 mg |
| $V_3S_4$@C-8 | 30 mg | 2.1 mg |

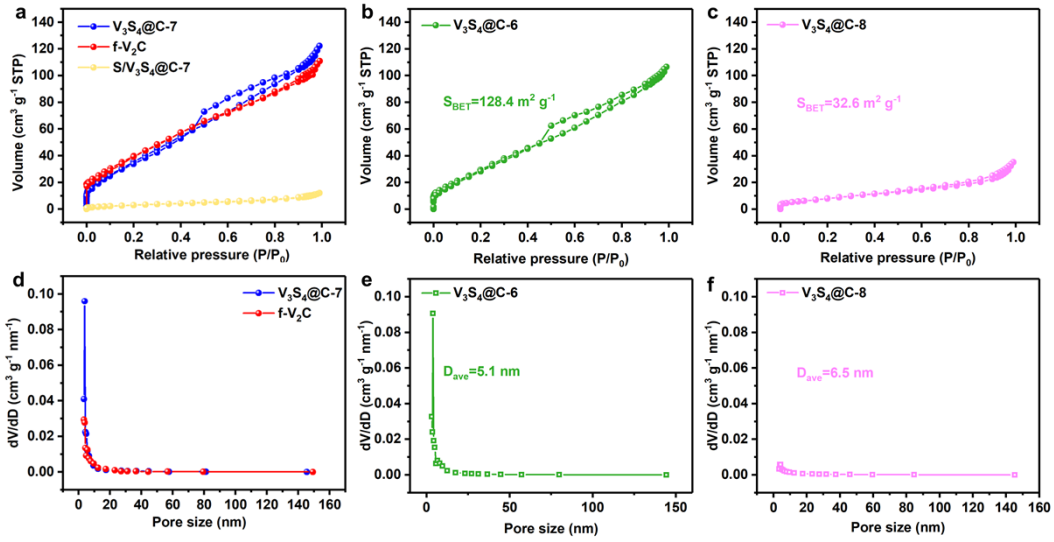


**Fig. S7** (a-c) Nitrogen sorption isothermal curves of (a) f-$V_2C$, $V_3S_4$@C-7, and S/$V_3S_4$@C-7, (b) $V_3S_4$@C-6, and (c) $V_3S_4$@C-8. Pore distribution plots of (d) f-$V_2C$ and $V_3S_4$@C-7, (e) $V_3S_4$@C-6, and (f) $V_3S_4$@C-8.

**Table S2** Total pore volume, average pore size and BET SSA of the $V_3S_4$@C-6, $V_3S_4$@C-7, $V_3S_4$@C-8, f-$V_2C$, and S/$V_3S_4$@C-7.

| Materials | Pore volume ($cm^3\ g^{-1}$) | Average pore size (nm) | BET SSA ($m^2\ g^{-1}$) |
|---|---|---|---|
| $V_3S_4$@C-6 | 0.15 | 5.1 | 128.4 |
| $V_3S_4$@C-7 | 0.18 | 5.0 | 149.9 |
| $V_3S_4$@C-8 | 0.04 | 6.5 | 32.6 |
| f-$V_2C$ | 0.11 | 4.5 | 150.6 |
| S/$V_3S_4$@C-7 | 0.01 | 4.1 | 11.50 |

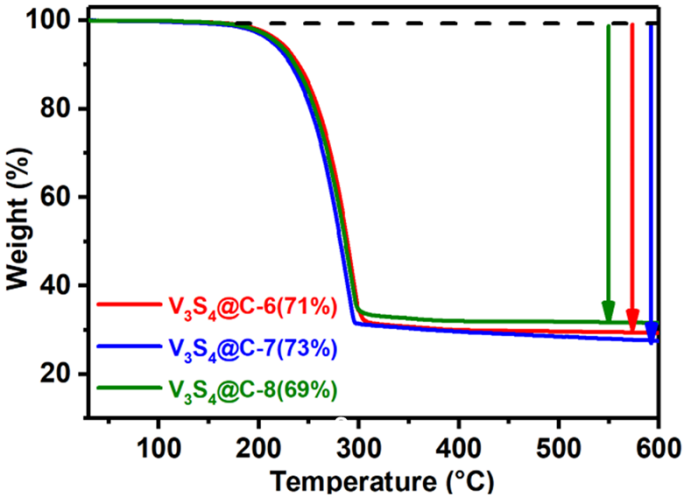


**Fig. S8** TG plots of $V_3S_4$@C-6, $V_3S_4$@C-7 and $V_3S_4$@C-8 as indicated.

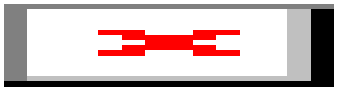

**Fig. S9** Equivalent circuit mode used to fit the EIS spectra of the S/$V_3S_4$@C-6, S/$V_3S_4$@C-7 and S/$V_3S_4$@C-8.

**Table S3** Fitted impedance parameters of different electrodes

| Electrodes | $R_s$ (Ω) | $R_{ct}$ (Ω) |
|---|---|---|
| V-6 | 1.9 | 90.6 |
| V-7 | 1.6 | 117.9 |
| V-8 | 1.9 | 70.3 |

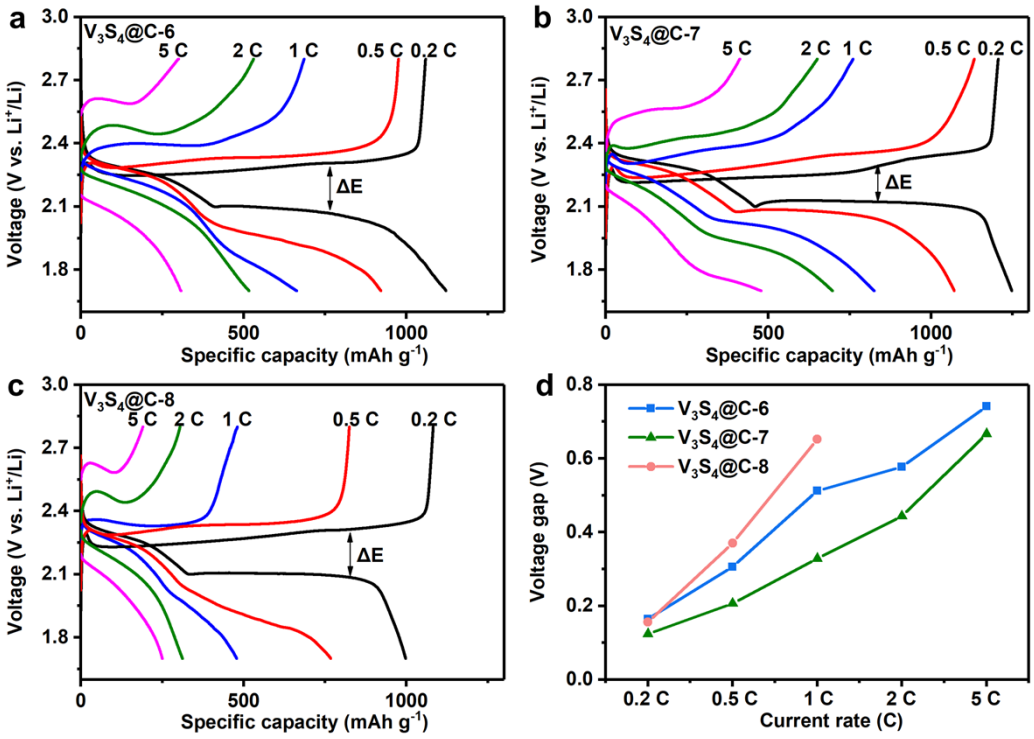


**Fig. S10** Selected charge and discharge voltage profiles (a) S/$V_3S_4$@C-6, (b) S/$V_3S_4$@C-7 and (c) S/$V_3S_4$@C-8, respectively; (d) Voltage gap between charge and discharge platforms at different current densities for the three electrodes as indicated.

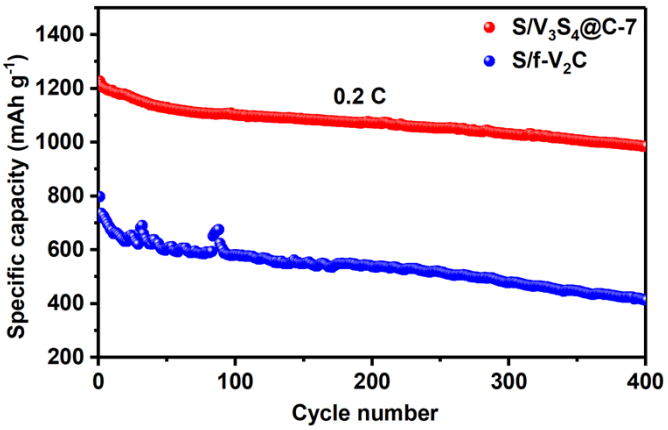


**Fig. S11** Cycling performance of $S/V_3S_4$@C-7 and S/f-$V_2C$ at 0.2 C.

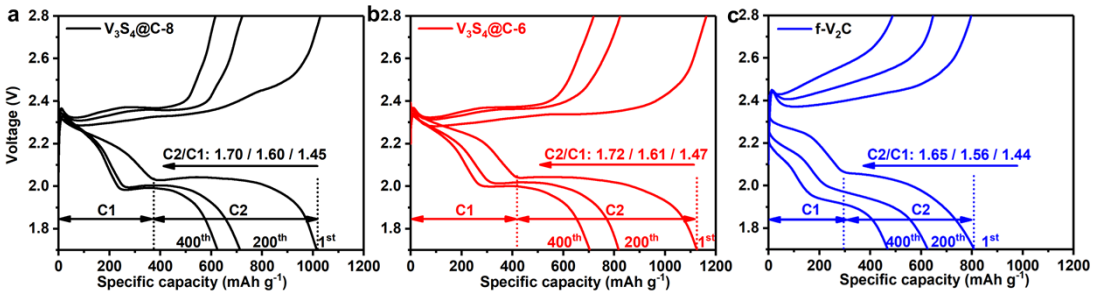


**Fig. S12** Charge/discharge plots (0.2 C) of (a) S/$V_3S_4$@C-8, (b) S/$V_3S_4$@C-6 and (c) S/f-$V_2C$ for the 1$^{st}$, 200$^{th}$ and 400$^{th}$ cycles as indicated.

**Table S4** Comparison of battery performance of $S/V_3S_4$@C-7 and other cathodes (1C = 1650 mA $g^{-1}$)

| Electrodes | Areal sulfur loading (mg $cm^{-1}$) | Performance (mAh $g^{-1}$) | Cycle number | Reference |
|---|---|---|---|---|
| $S/V_3S_4$@C-7 | 2.3<br>4.2 | 611.4 at 1C<br>389.3 at 1C | 500 | This work |
| S@$MnCo_2O_4$/CNT | 2.5 | 601 at 1C | 200 | [1] |
| S@$NiCo_2O_4$/CC | 3.5 | 660 at 0.2C | 200 | [2] |
| $NiFe_2O_4$@S/C | 3.0 | 790 at 0.3C | 200 | [3] |
| Crumpled N-$Ti_3C_2T_x$/S | 5.1 | 551 at 0.2C | 100 | [4] |
| S/Co-NBC | 1.4 | 440 at 0.5C | 500 | [5] |
| SnS@C/S | 1.5 | 513 at 0.5C | 600 | [6] |
| $TiO_2$-$Ni_3S_2$ | 3.9 | 504 at 0.3C | 500 | [7] |
| 3DRGO/NC-BL@S | 2.0 | 644 at 0.5C | 500 | [8] |
| Co-$NiSe_2$@NC | 1.5 | 544.6 at 0.5C | 200 | [9] |

**Reference**


[1] J. Sivaraj, D. Bosubabu and K. Ramesha, *Energy Fuels*, 2022, **36**, 2202.

[2] S. Chen, J. Zhang, Z. Wang, L. Nie, X. Hu, Y. Yu and W. Liu, *Nano Lett.*, 2021, **21**, 5285.

[3] H. Wang, N. Zhang, Y. Li, P. Zhang, Z. Chen, C. Zhang, X. Qiao, Y. Dai, Q. Wang and S. Liu, *J. Phys. Chem. Lett.*, 2019, **10**, 6518.

[4] Y. Wu, Y. Sun, J. Zheng, J. Rong, H. Li and L. Niu, *J. Phys. Energy*, 2021, **3**, 032009.

[5] Z. Zhang, D.-G. Xiong, A.H. Shao, X.-Y. Huang, Y. Huang, J. Yu, J.X. Cai and Z.Y. Yang, *Carbon*, 2020, **167**, 918.

[6] Y. Huang, S. Chen, Z. Wu, J. Wang, Q. Deng, Z. Zeng and S. Deng, *Electrochim. Acta*, 2020, **343**, 136148.

[7] R. Wang, C. Luo, T. Wang, G. Zhou, Y. Deng, Y. He, Q. Zhang, F. Kang, W. Lv and Q.H. Yang, *Adv. Mater.*, 2020, **32**, 2000315.

[8] R. Lu, M. Cheng, L. Mao, M. Zhang, H. Yuan, K. Amin, C. Yang, Y. Cheng, Y. Meng and Z. Wei, *EcoMat*, 2020, **2**, e12010.

[9] T. Chen, Z. Shang, B. Yuan, N. Wu, M. Abuzar, J. Yang, X. Gu, C. Miao, M. Ling and S. Li, *Energy Technol.*, 2020, **8**, 2000302.